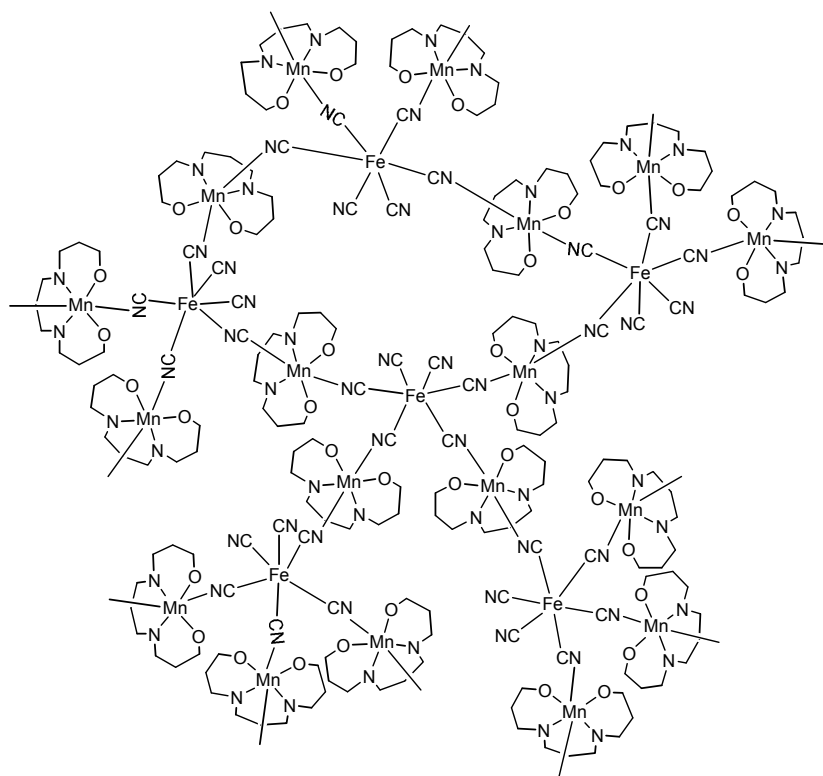


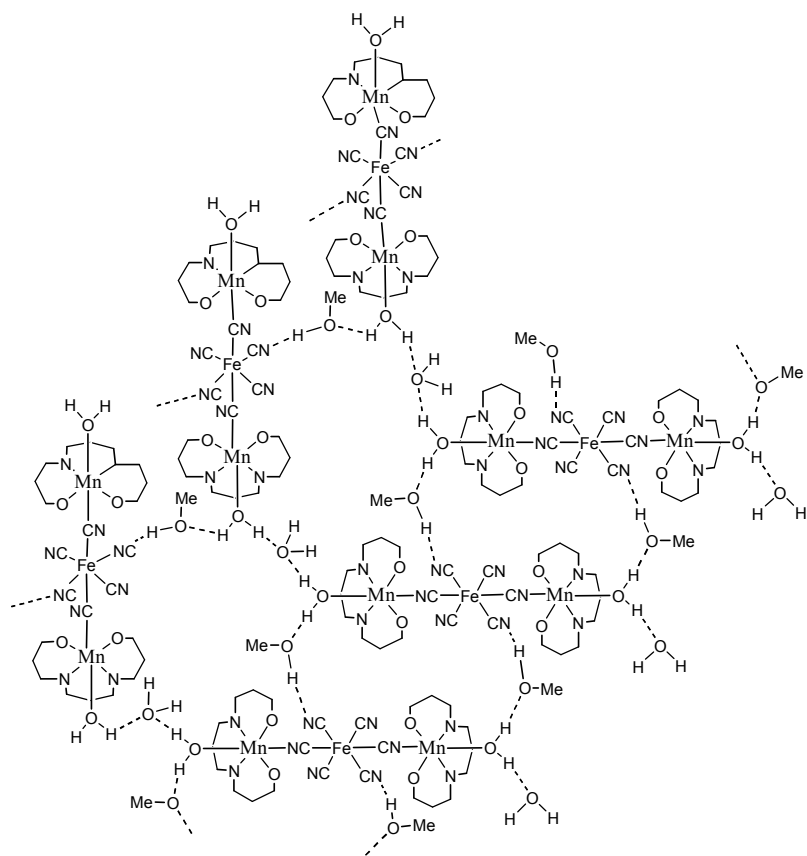
Supplementary materials

Table S1: U-B3LYP data computed for **1** and **3**.

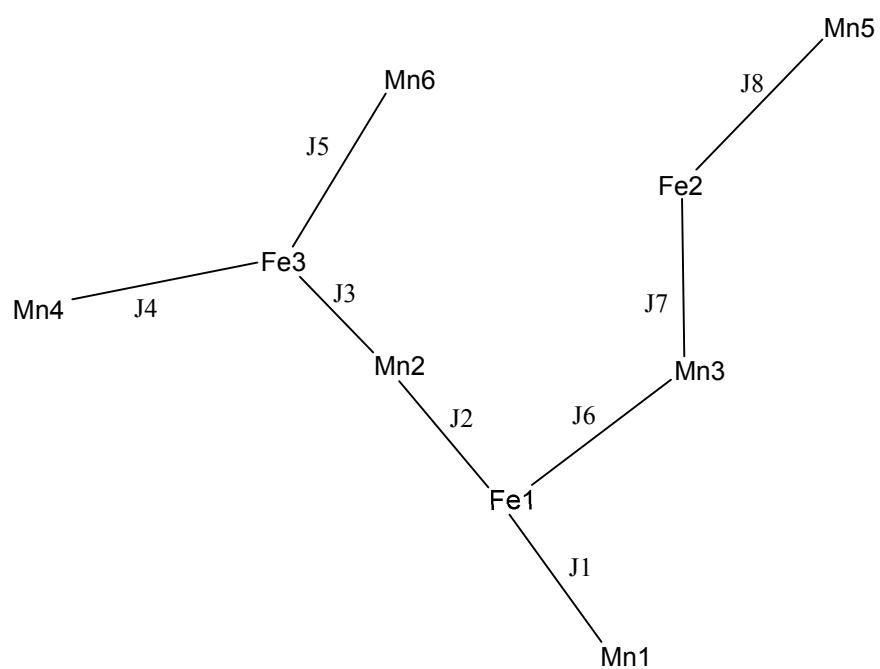
	1		3	
Spin population	BHS	BLS	BHS	BLS
Mn	3.8720	3.8775	3.8587	3.8519
Fe	1.1518	-1.1150	1.1441	-1.1211
Mn	3.8776	3.8800	3.8597	3.8686
$\langle S^2 \rangle$	24.8620	16.8578	24.8550	15.8303
E (a.u.)	-3652.8989513	-3652.8990621	-4092.9508976	-4092.9507293



Scheme S1 Schematic diagram of **1** and **2**.



Scheme S2 Schematic diagram of **3**.



Scheme S3. The eight different magnetic coupling pathways in compound **2**.

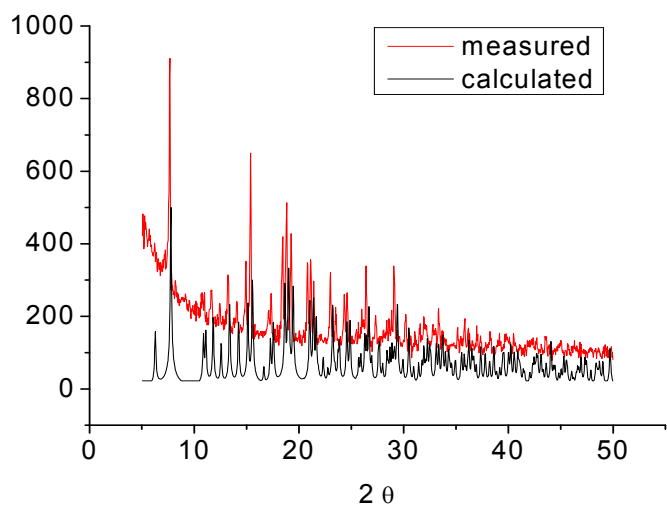


Figure S1. Powder XRD pattern for **1**.

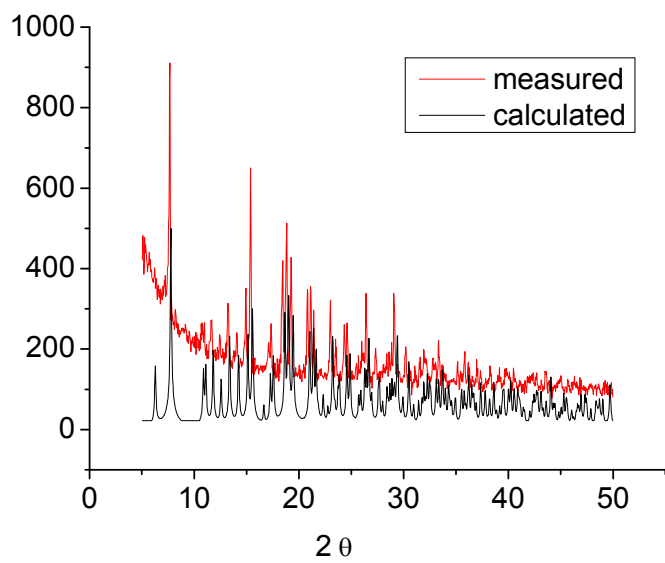


Figure S2. Powder XRD pattern for **2**.

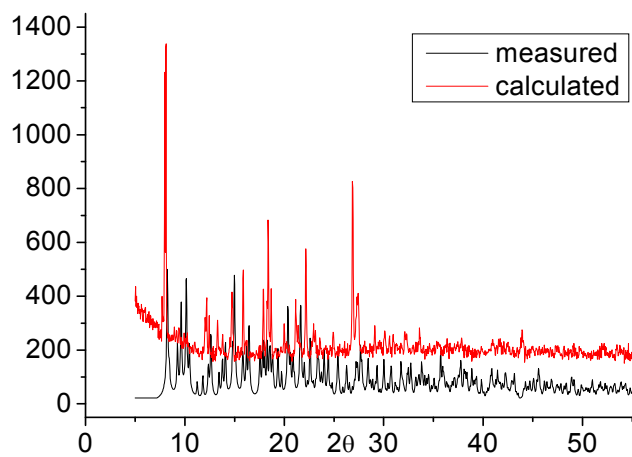


Figure S3. Powder XRD pattern for **3**.

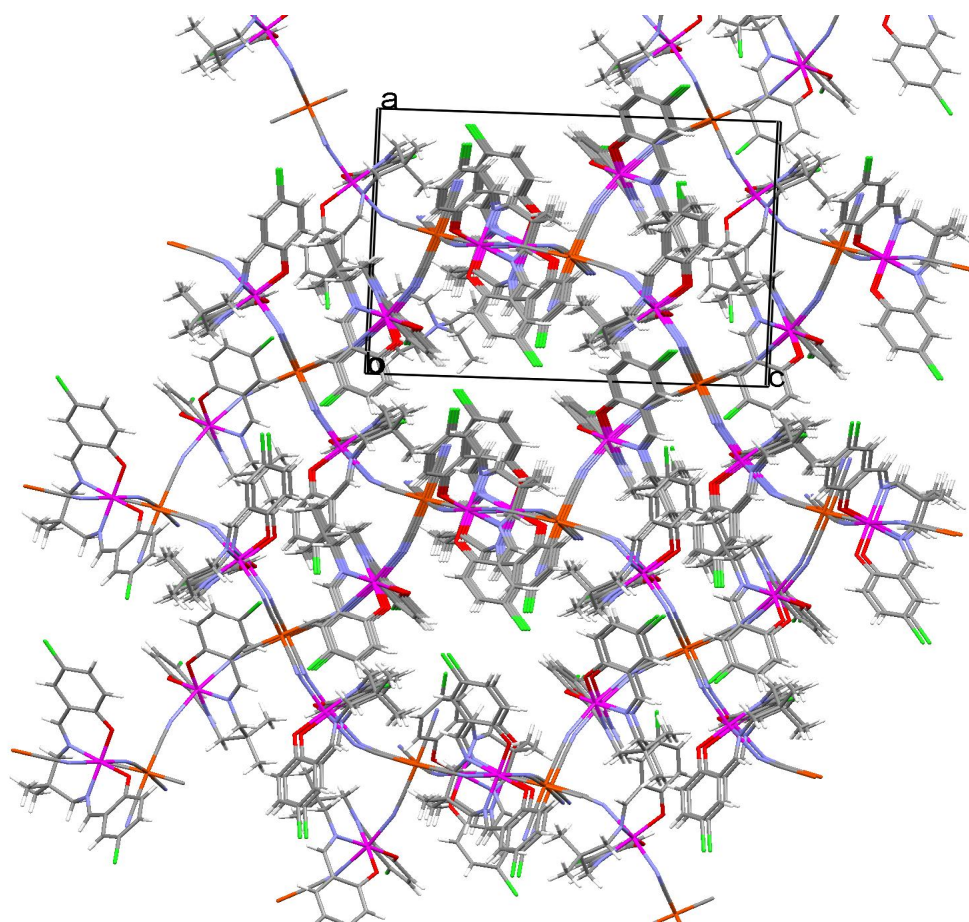


Figure S4. A three-dimensional network structure in the ac-plane of the compound **1**. $[\text{NEt}_4]^+$ and solvent molecules have been omitted for clarity.

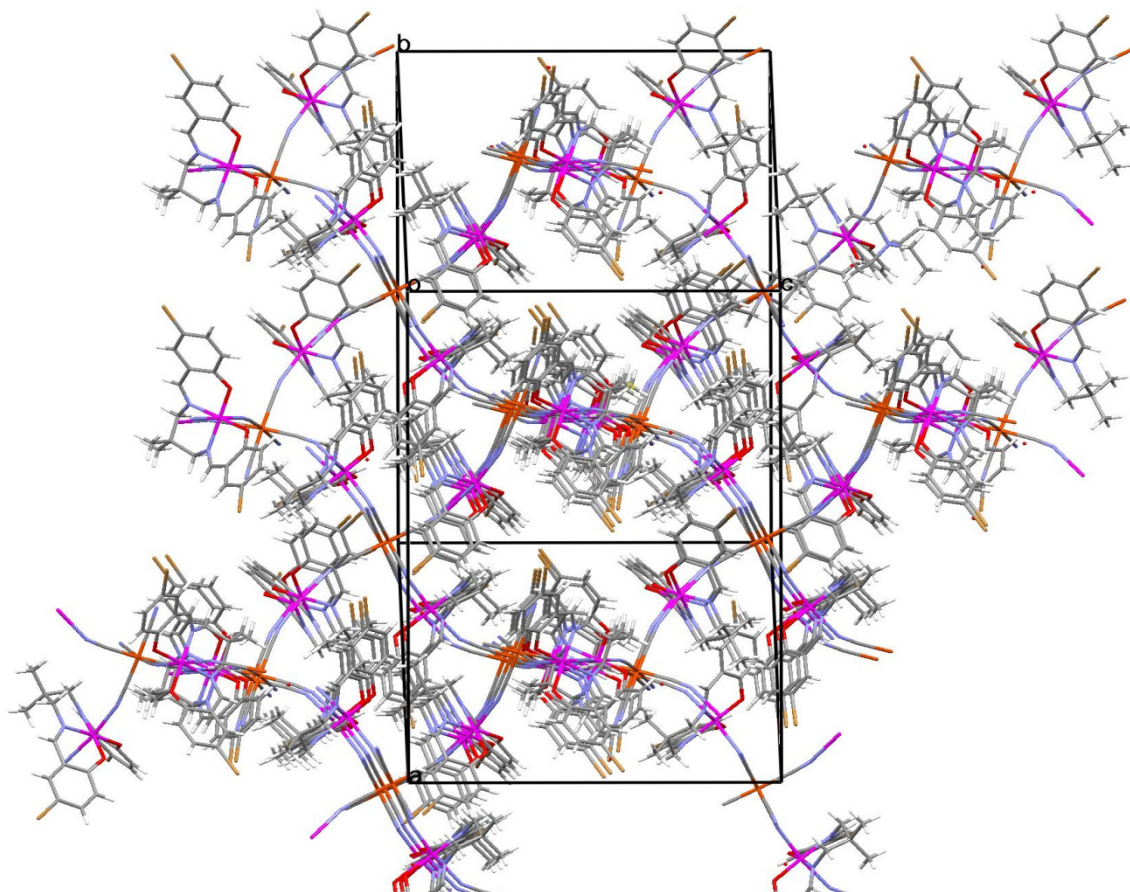


Figure S5. A three-dimensional network structure of the compound **2**. $[\text{NEt}_4]^+$ and solvent molecules have been omitted for clarity.

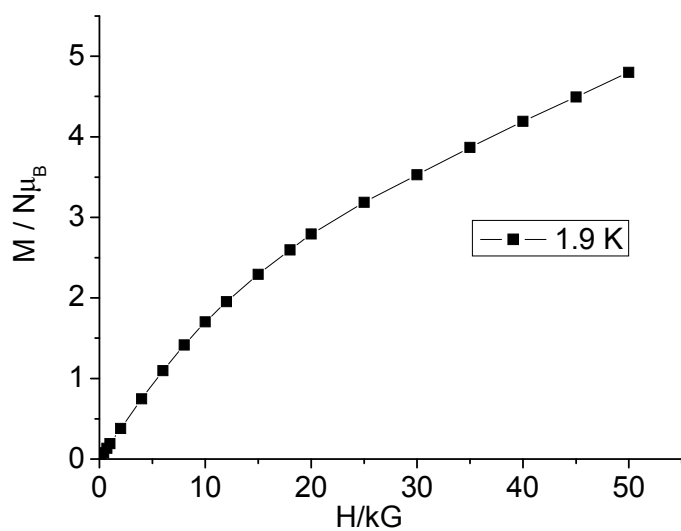


Figure S6. Magnetization as a function of the applied magnetic field up to 50 kOe for **1**, performed at 1.9 K.

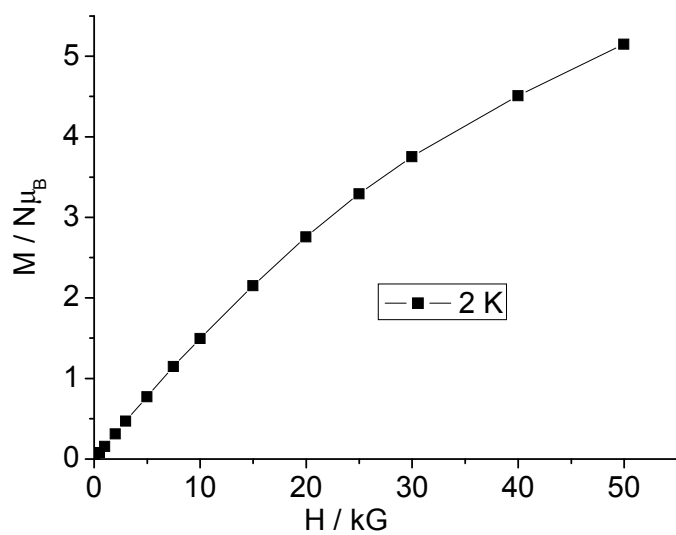


Figure S7. Magnetization as a function of the applied magnetic field up to 50 kOe for **2**, performed at 2 K.

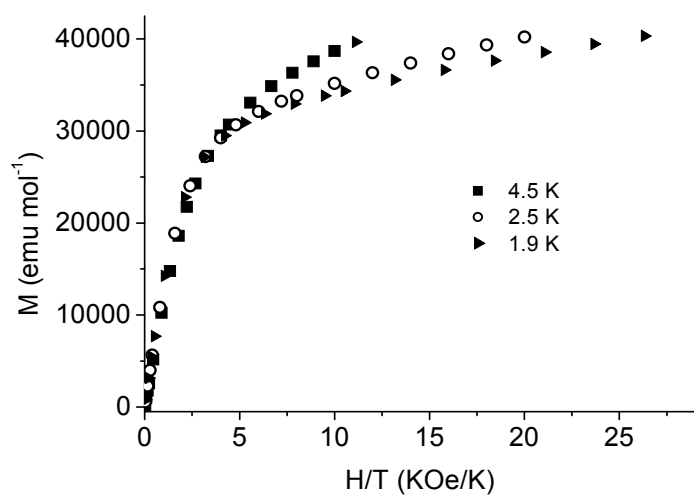


Figure S8. Magnetization as a function of the H/T ratio for **3**, measured at three different temperatures.

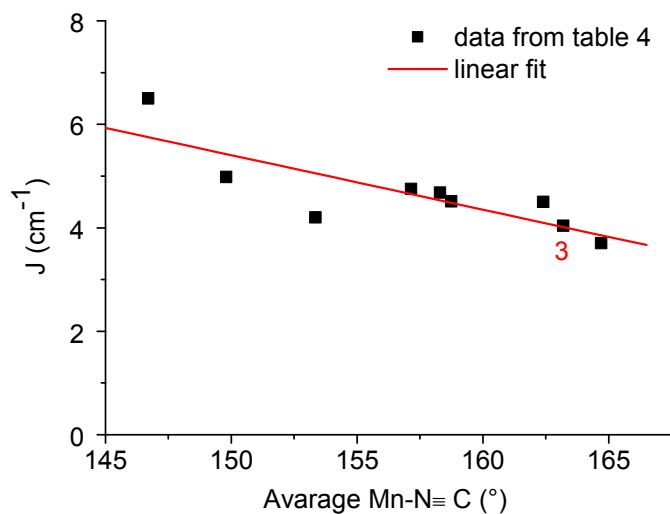


Figure S9. A plot of Mn-N≡C (°) bond angles vs. the exchange interactions (J); squares are literature data listed in Table 4